

A LABORATORY EXPERIMENT IN ACCELERATION-SKEWED OSCILLATORY SHEET FLOW

Paulo Silva(1), Tiago Abreu(2) , Gerben Ruessink(3), Hervé Michallet(4), Francisco Sancho(5), Dominic van der A(6), Jebbe van der Werf(7), Jan Ribberink(8), Tom O'Donoghue(6) & André Temperville(4),

(1) University of Aveiro, Physics Department & CESAM, Portugal, E-mail: psilva@ua.pt

(2) Polytechnic Institute of Viseu, Civil Eng. Department, Portugal, E-mail: tabreu@estv.ipv.pt

(3) Utrecht University, Department of Physical Geography, The Netherlands, E-mail: g.ruessink@geo.uu.nl

(4) University of Grenoble - LEGI, France, E-mail: herve.michallet@hmg.inpg.fr,
andre.temperville@wanadoo.fr

(5) LNEC National Civil Eng. Laboratory, Portugal, E-mail: fsancho@lnec.pt

(6) University of Aberdeen, School of Eng., United Kingdom, E-mail: d.a.vandera@abdn.ac.uk,
t.odonoghue@abdn.ac.uk

(7) Deltares, The Netherlands, E-mail: Jebbe.vanderWerf@deltares.nl

(8) Water Engineering and Management. University of Twente, The Netherlands, E-mail:
J.S.Ribberink@ctw.utwente.nl

New experiments of sand transport under sheet flow conditions were carried out in the Large Oscillating Water Tunnel (LOWT) of Deltares. In this work the measured net sediment transport rates, the structure of the sheet flow layer and sediment flux vertical profiles along the oscillatory wave cycle are presented and the importance of acceleration skewness on the sediment transport processes is analyzed and discussed.

1. INTRODUCTION

In the last trimester of 2007, a new set of laboratory experiments involving measurements of sand transport processes over horizontal, mobile sand beds was carried out in the Large Oscillating Water Tunnel (LOWT) of Deltares. The experiment, denominated TRANSKEW, provides details of the flow and bed conditions under oscillatory skewed waves, in the sheet flow regime for a well-sorted sand ($d_{50} = 0.20$ mm).

This new dataset allows the study of the effects of acceleration- and velocity-skewed flows with and without opposing net currents on sediment transport processes, providing results within an area that was recently identified as requiring further research (van der Werf et al., 2009). Furthermore, the data contribute to the validation and further development of sand transport models (Abreu et al., 2008).

The experimental facility consists of a U-tube construction with a rectangular horizontal test section (14 m long, 0.3 m wide and 1.1 m height with a 0.3 m thick sand bed) and two cylindrical risers at either end. A piston system housed in one of the cylinders is capable to generate near bottom horizontal velocities in the test section that correspond to full-scale wave conditions in the near shore-zone. The LOWT is fitted with a recirculation system that enables the generation of a mean current that can be superimposed on the oscillatory flow (see Ribberink & Al-Salem, 1994, for details). The wave forcing was imposed through a simple analytical formulation that reproduces a skewed, nonlinear wave form, as described in Abreu et al. (*sub judice*). Beside its application for the wave forcing in experimental facilities, this formulation can be used in many other engineering applications that require the use of a representative wave form (e.g., Ruessink et al., 2009).

2. EXPERIMENTAL CONDITIONS AND NET TRANSPORT RATES

In the first set of the experiments, the mean values of the net sand transport rates, q_s , were measured (Silva et al., 2008). The test conditions consisted of a repetition of regular oscillatory flows with the

same velocity root-mean-square value ($U_{rms} \approx 0.9 \text{ m/s}$) and two different wave periods ($T = 7$ and 10 s). Three major flow categories were considered: series A consisted of regular oscillatory flows with different degrees of acceleration skewness, $\beta = a_{max}/(a_{max} - a_{min})$, where a is the acceleration; Series B considered acceleration-skewed oscillatory flows with a collinear net current (U_0), opposing the (implied) wave direction; and Series C consisted of oscillatory flows with both velocity and acceleration skewness. The velocity skewness is characterized by $R = u_{max}/(u_{max} - u_{min})$, where u is the flow velocity. Table 1 lists the characteristics of the oscillatory flow measured 30 cm above the bed. (note that for oscillatory flow without acceleration and velocity skewness $\beta = 0.5$ and $R = 0.5$)

Table 1. Hydraulic characteristics obtained for the test conditions.

Condition	U_{rms} (m/s)	β	R	T (s)	U_0 (m/s)
A1	0.90	0.64	0.50	7	0.00
A2	0.88	0.63	0.49	10	0.00
A3	0.88	0.72	0.50	7	0.00
A4	0.86	0.72	0.49	10	0.00
B1	0.89	0.64	0.50	7	-0.22
B2	0.88	0.64	0.50	7	-0.44
B3	0.86	0.71	0.50	7	-0.22
B4	0.86	0.71	0.51	7	-0.44
C1	0.86	0.61	0.59	7	0.00
C2	0.94	0.60	0.59	10	0.00
C3	0.87	0.53	0.59	7	0.00

The net total transport rates were calculated by applying a mass conservation technique and are shown in Figure 1 as a function of β , R and U_0 . The acceleration skewness produces a net transport in the (positive) wave direction. The values of q_s are proportional to β and R . In the case of a counter current, the amount of sediment transported in the negative direction of the mean current is reduced when the value of β increases.

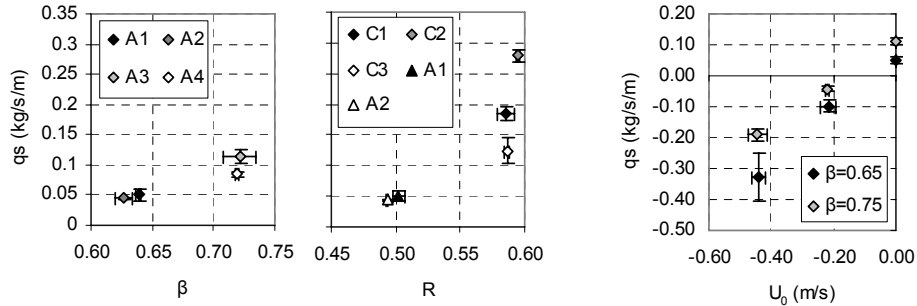


Figure 1 – Net transport rates and standard deviations. Influence of β , R and U_0 on q_s .

3. SHEET FLOW LAYER STRUCTURE AND SEDIMENT FLUXES

In the second set of the experiments several instruments were deployed within the LOWT to obtain detailed measurements of the intra-wave velocities and concentrations within the suspension and sheet flow layers (SFL) for the tests conditions A1, A3, B2, B4 and C1. Herein we only present the results concerning condition A3.

Silva et al. (2009) analysed the data gathered by two different devices, an Acoustic Doppler Velocity Profiler (ADVP) and two Conductivity Concentration Meters (CCM), to study the SFL structure within the wave cycle. The ADVP enables to deduce velocities along the receivers beam axis over a whole profile with a vertical resolution of about 3 mm. Also, the intensity of the backscattered acoustic signal over the depth can be used to determine the bed position and the top of the sheet-flow layer. The CCM probes measured the conductivity change of a sand-water mixture and were then converted to sediment concentrations. The CCM measures large concentrations, more specifically, in the range of 100-1600 g/l. The estimates of the upper and lower SFL bounds along the oscillatory motion agree quite well using both ADVP and CCM data, as shown in Figure 2 for test A3. The results illustrate the development of the SFL during the wave cycle: as the velocity increases from zero

values, at each flow reversal, sediment particles are mobilized from the bed, thus causing local erosion associated with a deepening of the bed level and an increase in the erosion depth. These particles are entrained into the flow above the initial bed level ($z=0$) causing an increase of sediment concentration at those levels and, consequently, raising the top level of the SFL, defined as the height where phase-average $C = 8\%$ vol. (~ 210 g/l). When the magnitude of the velocity decreases, the processes that sustain the sediment particles either in the sheet flow or in the suspension layer tend to vanish, and sediment particles have a tendency to settle down to the bed, causing a decrease in the SFL thickness. The SFL thickness is higher under the crest than under the trough, although the maximum velocities under the wave crest and trough are equal, and this seems related with the enhanced bed shear stress (Ruessink et al., 2008). The data also shows that under the largest acceleration values, i.e., when the velocity changes rapidly from the offshore negative maximum to an onshore positive maximum, the SFL remains thicker than at the opposite on-offshore flow reversal where much smaller flow accelerations are found.

The time-varying sediment fluxes within the SFL were obtained by combining the measured concentration values with the velocity of the sand particles. Abreu et al. (2009) applied a new methodology for the estimation of the grain velocity inside the sheet flow layer from the measurements of the two CCMs by combining cross-correlation techniques (McLean et al., 2001) with wavelet multilevel decomposition (Mallat, 1999; Franca and Lemmin, 2006). This methodology yields quite consistent velocity measurements over the entire sheet flow layer and for most of the wave phases. The velocities provided by the ADVP were simultaneously analysed near the sand bed (at $z=0$, 3 and 6 mm) and are in good agreement with the velocities estimated from the cross correlation technique. These velocity measurements allowed the estimation of the sediment fluxes. At the levels below $z=0$, the instantaneous velocities were obtained by interpolating the ADVP measurements and imposing a null velocity at the erosion depth for each wave phase.

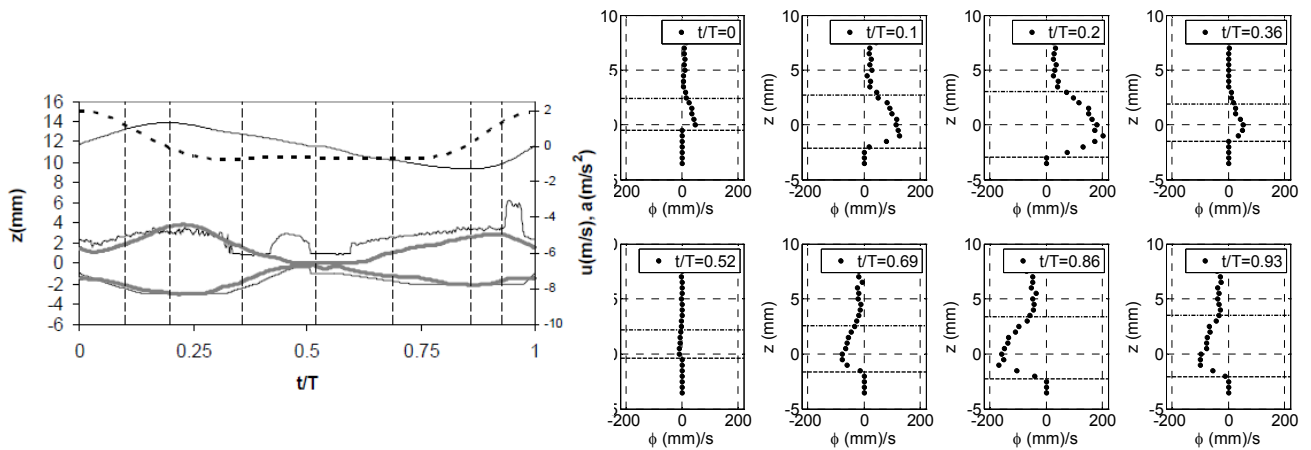


Figure 2 – Experimental condition A3: a) time-series of the measured (ensemble-averaged) free-stream velocity (solid line) and acceleration (dashed line); b) lower and upper levels of the SFL computed from CCM (black solid lines) and ADVP (grey solid lines); c) vertical profiles of sediment flux at select phases

Figure 2c) presents the computed vertical sediment flux profiles at select phases as indicated in Figure 2a). The horizontal lines mark the erosion depth and the upper limit of the SFL for each wave phase presented. The values above the top of the SFL should be taken with caution, since the related concentrations are generally below 100 g/l, that is out of the range of accurate measurements with the CCM probes. The largest fluxes occur at times of maximum free-stream velocity and are higher for the onshore maximum velocity. The bed shear stress (not shown) also depicts an asymmetry with higher values during onshore flow. At $t/T = 0$ the depth-averaged flux is positive while it is close to zero at the flow reversal $t/T = 0.52$. This is in agreement with the results for the SFL thickness around flow reversal as described above, and supports the existence of phase-lag effects between the sediment particles and the flow at $t = 0$ which provides an additional means for onshore transport. These non-steady effects are also evident in the A1, B2 and B4 results.

The depth-integrated and wave-averaged transport in the SFL accounts for, approximately, 75% of

the measured net total transport, which also means that the net suspended transport is in the same direction as in the SFL underneath. A similar conclusion is attained for the A1, B2 and B4 tests, however the SFL transport to total transport ratio are estimated about 53%, 40% and 90% , respectively. For the C1 test the SFL net transport exceeds the measured net total transport which means that the contribution of the suspended layer is negative.

4. CONCLUSIONS

The present results show that flow acceleration skewness induces a net sediment transport in the direction of largest acceleration. This is believed to be the result of an increased bed shear stress under the wave crest, mobilizing more sediment from the bed and increasing the SFL thickness, and also with an additional contribution from phase lag effects occurring under the largest acceleration values. In the experiments with a counter current, the acceleration-skewness induced reduces the amount of sediment transported in the negative direction of the mean current. For the test C1, with velocity and acceleration skewness, the acceleration skewness contributes to about 30% of the total net transport rate.

ACKNOWLEDGEMENT

This work has been supported by European Community's Sixth Framework Programme through the grant to the budget of the Integrated Infrastructure Initiative HYDRALAB III within the Transnational Access Activities, Contract no. 022441.

REFERENCES

- Abreu, T., Silva, P.A. and Sancho, F. 2008. Comparison of Sediment Transport Formulae Regarding Accelerated Skewed Waves, *Poster Proc. 31st Int. Conf. on Coastal Eng., ASCE, Hamburg*, pp. 145-155.
- Abreu, T., Franca, M.J., Silva, P.A. and Sancho, F. 2009. Estimation of sediment particle velocities in sheet flow: cross-correlation and wavelet analysis, *Proc. 6 IAHR River, Coastal and Estuarine Morphodynamics*, pp. 1051-1056
- Abreu, T., Silva, P.A., Sancho, F., Temperville, A. 2009. Analytical approximate wave form for asymmetric waves, *Coastal Engineering, sub judice*
- Franca, M.J. and Lemmin, U. 2006. Detection and reconstruction of coherent structures based on wavelet multiresolution analysis, *River Flow 2006, Lisbon*
- McLean, S.R., Ribberink, J.S., Dohmen-Janssen, C.M. and Hassan, W.N. 2001. Sand transport in oscillatory sheet flow with mean current. *J. Waterway Port Coast. Ocean Eng., ASCE, 127(3)*, pp.141–51.
- Mallat S. 1999. A wavelet tour of signal processing, *Academic Press, San Diego (USA)*
- Silva, P., Abreu, T., Freire, P., Kikkert, G., Michallet, H., O'Donoghue, T., Plecha, S., Ribberink, J., Ruessink, G., Sancho, F., Steenhauer, K., Temperville, A., Van der A., D. and Van der Werf, J. 2008. *Sand transport induced by acceleration-skewed waves and currents – The TRANSKEW project, PECS08 – Physics of Estuaries and Coastal Seas, Liverpool*
- Silva, P.A., Abreu, T., Michallet, H., Hurther, D., Sancho, F. 2009. Sheet flow layer structure under oscillatory flows, *Proc. 6 IAHR River, Coastal and Estuarine Morphodynamics*, pp. 1057-1062.
- Ribberink, J.S. and Al-Salem, A. 1994. Sediment transport in oscillatory boundary layers in cases of rippled bed and sheet flow. *J. Geophys. Res., 99 (C6)*, pp. 12707-12727.
- Ruessink, G.B., Michallet, H., Hurther, D., Silva, P. A., 2008. Observations of intra-wave suspended sediment transport under acceleration-skewed oscillatory flow. *Eos Trans. AGU, 89(53)*, Fall Meet. Suppl., Abstract OS21E-1207.
- Ruessink, B.G., van den Berg, T.J.J., van Rijn, L.C., 2009. Modeling sediment transport beneath skewed-asymmetric waves above a plane bed. *J. Geophys. Res. 114*, C11021, doi:10.1029/2009JC005416.
- van der Werf, J., Schretlen, J., Ribberink, J., O'Donoghue, T., 2009. Database of full-scale laboratory experiments on wave-driven sand transport processes. *Coast. Eng., 56*, pp. 726–732